LETTERS

# Electromagnetically induced transparency with tunable single-photon pulses

M. D. Eisaman[1], A. André[1], F. Massou[1], M. Fleischhauer[1,2,3], A. S. Zibrov[1,2,4] & M. D. Lukin[1]

**Techniques to facilitate controlled interactions between single photons and atoms are now being actively explored[1–7]. These techniques are important for the practical realization of quantum networks, in which multiple memory nodes that utilize atoms for generation, storage and processing of quantum states are connected by single-photon transmission in optical fibres[1,2]. One promising avenue for the realization of quantum networks involves the manipulation of quantum pulses of light in optically dense atomic ensembles using electromagnetically induced transparency (EIT, refs 8, 9). EIT is a coherent control technique that is widely used for controlling the propagation of classical, multi-photon light pulses[10–14] in applications such as efficient nonlinear optics[15]. Here we demonstrate the use of EIT for the controllable generation, transmission and storage of single photons with tunable frequency, timing and bandwidth. We study the interaction of single photons produced in a 'source' ensemble of $^{87}$Rb atoms at room temperature with another 'target' ensemble. This allows us to simultaneously probe the spectral and quantum statistical properties of narrow-bandwidth single-photon pulses, revealing that their quantum nature is preserved under EIT propagation and storage. We measure the time delay associated with the reduced group velocity of the single-photon pulses and report observations of their storage and retrieval.**

The basic idea of our experiments is illustrated in Fig. 1a. Single photons are prepared in an ensemble of room-temperature $^{87}$Rb atoms (called the 'source ensemble') by first creating a single spin excitation via Raman scattering combined with single-photon detection, and later converting this atomic excitation 'on demand' into a single photon propagating in an optical fibre[3,4,16–21]. Successful preparation of the single-photon pulse is conditional on detecting a single Raman-scattered photon[16,17]. The single photons are directed via an optical fibre to a second atomic ensemble ('target ensemble'), where their controlled interaction with coherently driven atoms is studied by combining EIT-based high-resolution spectroscopy and photon-counting measurements.

We begin by describing our source of narrow-bandwidth, frequency-tunable single photons with properties matching those of narrow atomic resonances[16,17]. As illustrated in Fig. 1a, the source ensemble is initially prepared in the ground state $|g\rangle$. Atomic spin excitations to the state $|s\rangle$ are produced via spontaneous Raman scattering, induced by a laser beam referred to as the write laser. In this process, correlated pairs of frequency-shifted photons (so-called Stokes photons) and flipped atomic spins are created (corresponding to atomic Raman transitions into the state $|s\rangle$). Energy and momentum conservation ensure that by detecting a Stokes photon emitted in a particular direction, the atomic ensemble is prepared in state with exactly one flipped spin quantum in a well-defined spin-wave mode. Conditioned upon detecting a single Stokes photon, the stored single spin-wave quantum is coherently converted into a single-photon anti-Stokes pulse by applying a second near-resonant laser beam (retrieve laser) after a controllable delay time[12]. The direction, bandwidth, and central frequency of the single-photon anti-Stokes pulse is determined by the direction, intensity and frequency of the retrieve laser[17]. Specifically, the retrieve laser controls the rate of retrieval and propagation of the anti-Stokes pulse, thereby controlling its duration, and consequently its bandwidth. The central frequency of the single-photon pulse differs from the frequency of the retrieve laser by a fixed amount given by the $|g\rangle$–$|s\rangle$ atomic transition frequency. We study the photon-number fluctuations in the Stokes and the anti-Stokes pulses using a Hanbury-Brown-Twiss-type setup, which allows us to measure normalized correlation functions $g^{(2)}(x,y) \equiv \langle :\hat{n}_x\hat{n}_y: \rangle / \langle \hat{n}_x \rangle \langle \hat{n}_y \rangle$, where $\hat{n}_i$ denotes the photon-number operator for field $i$, and :: denotes operator normal ordering[22,23].

To quantify the properties of the single-photon source, the target ensemble was first removed from the beam path. Figure 2 shows a measurement of the photon-number fluctuations of the anti-Stokes field conditioned on detecting a single Stokes photon, as a function of the detection probability $p\eta_S$ in the Stokes channel. (Here $p$ is the Raman excitation probability, and $\eta_S$ is the overall Stokes channel transmission.) The function $g^{(2)}(AS\|n_S = 1)$ (where $n_S$ is the number of detected Stokes photons; see Fig. 2) represents a measure of the photon-number fluctuations in the anti-Stokes pulses. An ideal single-photon source has no photon-number fluctuations ($g^{(2)}(AS\|n_S = 1) = 0$); for classical coherent states $g^{(2)}(AS\|n_S = 1) = 1$. In Fig. 2, $p\eta_S$ is varied by changing $p$ via the write laser intensity. As $p$ becomes much smaller than unity, we observe substantial suppression of the conditional intensity fluctuations in the anti-Stokes pulses ($g^{(2)} = 0.3 \pm 0.2$ for $p\eta_S = 0.06$ and $\eta_S = 0.27$) compared to the classical limit of unity. Typical conversion efficiencies of atomic excitations into anti-Stokes photons are 8–15%. These observations are in good agreement with a simple theoretical model[24] that considers realistic losses and background photons. The presence of loss on the Stokes channel means that detection of a single Stokes photon can result in more than one atomic excitation. Upon retrieval, this results in the undesired emission of more than one anti-Stokes photon. Even in the presence of loss, one can obtain almost perfect preparation of an atomic state with a single excitation by ensuring that the Raman excitation probability $p$ is much less than one. In this case, the probability of emitting two photons is suppressed by $p \ll 1$. This condition is satisfied when $p\eta_S \ll \eta_S$, in agreement with the experimental observations in Fig. 2.

We next consider the interaction of these non-classical anti-Stokes pulses with the optically dense target ensemble (Fig. 1). Usually such a medium simply absorbs the incoming light, reducing its intensity and destroying its quantum state. To restore transparency and control the light propagation, EIT is used. The essence of EIT,

[1]Physics Department, Harvard University, [2]Harvard-Smithsonian Center for Astrophysics, Cambridge, Massachusetts 02138, USA. [3]Fachbereich Physik, Technische Universität Kaiserslautern, D-67663 Kaiserslautern, Germany. [4]P. N. Lebedev Institute of Physics, Moscow, 117924, Russia.

illustrated on the right-hand side of Fig. 1a, is a strong coupling of an incident light pulse (anti-Stokes field in Fig. 1a) to a long-lived $|g\rangle$–$|s\rangle$ atomic coherence (spin wave), mediated by a coherent laser ('EIT control' laser). This control laser converts the incoming light pulse into a so-called 'dark' spin state, thereby eliminating dissipative absorption and substantially reducing its group velocity[25]. Note that EIT is effective only within a narrow range of frequencies associated with the spectral transparency window, which occurs when the frequency difference between the incident pulse and the control laser matches the frequency of the spin coherence.

The main idea behind our experimental implementation is to match the bandwidth and the central frequency of our single-photon source to the EIT transparency resonance of the target ensemble by tuning, respectively, the retrieve and the control laser intensities and frequencies[17]. The relative detuning between the retrieve and EIT control lasers is carefully controlled via acousto-optic modulators. Figure 3a shows the conditional probability of detecting an anti-Stokes photon transmitted through the target ensemble, $\langle n\rangle(AS\|n_S = 1)$, as a function of the two-photon detuning $\delta$ (the difference between the anti-Stokes/EIT control laser frequency difference, and the $|g\rangle$–$|s\rangle$ transition frequency). The clear resonance structure displays maximum transmission for $\delta = 0$. At this point, the central frequency of the single photons coincides with the EIT resonance window, resulting in a three-fold increase in transmission, which corresponds to 60% transmission of the incident pulse. The observed conditional probabilities can be used to quantify the correlations between the Stokes and anti-Stokes photon numbers using the normalized correlation function $R \equiv g^{(2)}(S, AS)^2/g^{(2)}(S, S)\, g^{(2)}(AS, AS)$. Classical fields must obey the Cauchy-Schwartz inequality $R \leq 1$; $R > 1$ indicates non-classical correlations[22]. For the data at $\delta = 0$, $R = 1.85 \pm 0.12$, including all background and dark counts; as $\delta$ is tuned away from zero in either direction, $R$ approaches the classical limit of unity.

Figure 3b shows the normalized photon-number fluctuations for the transmitted anti-Stokes field conditioned upon detection of $n_S = 1$ Stokes photon, $g^{(2)}(AS\|n_S = 1)$, versus $\delta$. We observe that $g^{(2)}(AS\|n_S = 1)$ retains its non-classical character upon transmission through the target ensemble only when near the centre of the EIT transparency window. The minimum measured value of $g^{(2)}(AS\|n_S = 1)$, occurring at $\delta = 0$ ($0.50 \pm 0.14$), is essentially equal to the value measured by removing the target ensemble from the beam path ($0.51 \pm 0.15$ for the displayed set of data). It is important to emphasize that the maximum of $\langle n\rangle(AS\|n_S = 1)$ and the minimum $g^{(2)}(AS\|n_S = 1)$ both occur at $\delta = 0$. As $\delta$ is tuned away from zero in either direction, $\langle n\rangle(AS\|n_S = 1)$ decreases while $g^{(2)}(AS\|n_S = 1)$ approaches the classical limit of unity, indicating that the non-classical nature of the anti-Stokes pulse is preserved only within the EIT transparency window[26]. The classical limit is also observed when the EIT control field is turned off. Likewise, $g^{(2)}(AS)$ obtained without conditioning exhibits no structure as a function of $\delta$ and again yields the classical limit of unity. Finally, we note that the photon-correlation data display a noise-enhancement feature on the

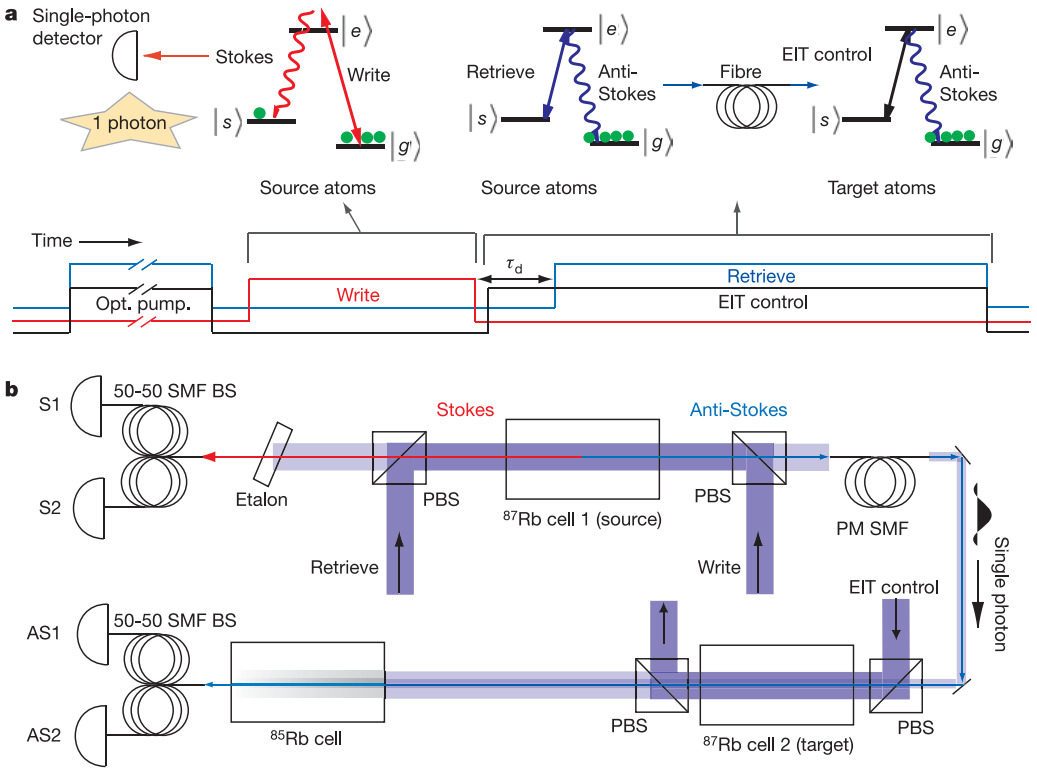


**Figure 1 | Experimental procedure and set-up. a**, Two ensembles of $^{87}$Rb atoms are used, the 'source' and 'target' ensembles. In zero magnetic field, the atoms can be pictured as a three-level atom, with: $|g\rangle = |5^2S_{1/2}, F = 1\rangle$, $|s\rangle = |5^2S_{1/2}, F = 2\rangle$, and $|e\rangle$ corresponds to $|5^2P_{1/2}, F' = 1\rangle$ and $|5^2P_{1/2}, F' = 2\rangle$. The write laser and the retrieve laser couple respectively the $|g\rangle$–$|e\rangle$ and $|s\rangle$–$|e\rangle$ transition of the source atoms; the EIT control laser couples the $|s\rangle$–$|e\rangle$ transition of the target atoms. **b**, The write and retrieve lasers counter-propagate[30] inside the magnetically shielded source ensemble, and the EIT control laser and anti-Stokes field co-propagate inside the magnetically shielded target ensemble. The write and retrieve lasers have a diameter of 1 mm and 3 mm respectively at the centre of the source ensemble. The single spatial mode defined by the detection fibres and optics has a diameter of 200 μm at the centre of the source ensemble. The etalon is used to reflect the fraction of the write laser not filtered by the polarizing beamsplitters, and the $^{85}$Rb cell is used to absorb the fraction of the retrieve/EIT control laser not filtered by the polarizing beamsplitters; this requires a retrieve and EIT control laser detuning of 400 MHz. The source and target ensembles are 4.5-cm-long isotopically pure $^{87}$Rb vapour cells with 7 torr and 8 torr respectively of neon buffer gas. PBS, polarizing beamsplitter; SMF, single-mode fibre; PM, polarization maintaining; BS, beamsplitter; and S1, S2 (or AS1, AS2) for avalanche photodetectors (APDs) for the Stokes (or anti-Stokes) channel.

high-frequency side of the EIT resonance.

These observations clearly demonstrate that EIT transmission preserves the non-classical statistics of the anti-Stokes pulses. The narrow resonances observed in transmission and photon-correlation data set an upper bound to the bandwidth (of order MHz) of the single-photon pulses generated in our experiments. To analyse these observations, we consider a theoretical model that describes the propagation of single photons of finite bandwidth and purity (that is, a finite probability of two-photon events) in an optically dense, coherently driven medium of three-level atoms. Included in this model is Doppler broadening, realistic detunings (resulting in an asymmetric spectrum), finite decay of the $|g\rangle$–$|s\rangle$ coherence, and spectrally broad noise associated with two-photon events. As shown in Fig. 3, the theoretical predictions are in good agreement with experimental observations. Note that this analysis shows that the spectral properties of single-photon and two-photon events in conditionally generated pulses differ. These effects, which involve the interplay between spectral and quantum-statistical properties, warrant further investigation.

One intriguing application of EIT involves the controllable delay of optical pulses by slowing their group velocity[10,11] and stopping their propagation[12–14,25]. Figure 4 presents an experimental realization of such controllable delay and storage for single-photon pulses. For these measurements, the single-photon anti-Stokes pulses were tuned to the centre of the EIT transmission window ($\delta = 0$); the retrieve laser was turned on for approximately 150 ns, generating anti-Stokes pulses of corresponding duration. Time-resolved measurements shown in Fig. 4a reveal substantial delay, relative to free-space propagation, of the conditionally generated anti-Stokes pulses upon transmission through the EIT medium. As shown in Fig. 4b, we observe delays up to 45 ns in our 4.5-cm-long ensemble, corresponding to single photon velocities of about $10^3\,\mathrm{km\,s^{-1}}$ (~0.003 times the speed of light in vacuum). In Fig. 4a, the observed delay of 40 ns corresponds to a substantial fractional delay of about 30% when compared to the 140 ns full-width at half-maximum of the reference pulse.

Figure 4c demonstrates that a fraction of the incoming single-photon pulses can be stored by dynamically reducing the single-photon group velocity to zero. This is accomplished by turning off the EIT control laser as the anti-Stokes pulse propagates in the target ensemble. The stored fraction is released when the control laser is turned back on[12–14]. Figure 4d shows the conditional storage and retrieval probability as a function of storage time. Storage and retrieval of up to 10% of the incoming pulse was observed at short storage times; retrieved pulses were observed for times up to a few microseconds, limited by atomic diffusion in the target ensemble. Even with these limited efficiencies, the retrieved pulses preserve some non-classical features after considerable storage intervals. For example, for a storage time of 0.5 μs, we deduce $R = 1.08 \pm 0.01 > 1$. The storage and retrieval efficiency could be improved by, for example, increasing the optical depth or utilizing an optical cavity with modest finesse[27]. The storage times could be considerably extended by reducing the effect of atomic diffusion, either by expanding the detection-mode diameter, working with ultra-cold atoms in dipole traps or optical lattices, or using a doped solid[14]. A factor of ten increase in the detection-mode diameter should extend storage times to a fraction of a millisecond[12].

These results demonstrate that EIT represents a very effective technique for generation and controlled propagation of narrow-bandwidth single-photon light pulses in optically dense atomic

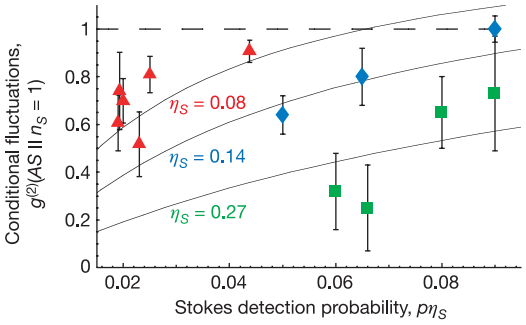


**Figure 2 | Observation of conditional single-photon generation.** Anti-Stokes fluctuations, conditioned on detection of a single Stokes photon, are characterized by the correlation function $g^{(2)}(AS||n_S = 1) = \langle \hat{n}_{AS1}\hat{n}_{AS2}\rangle / \langle \hat{n}_{AS1}\rangle\langle \hat{n}_{AS2}\rangle$, where $(\hat{n}_{AS1}, \hat{n}_{AS2})$ is the number operator for detector (AS1, AS2), see Fig. 1b. The dotted line represents the classical limit of $g^{(2)}(AS||n_S = 1) = 1$. Measurements are shown for three values of the Stokes channel transmission: $\eta_S = 0.08$ (red triangles), $\eta_S = 0.14$ (blue diamonds) and $\eta_S = 0.27$ (green squares). Solid lines represent a theoretical model[24] for $\eta_S$ equal to 0.08, 0.14 and 0.27 respectively. For this data, source ensemble temperature ~26 °C (estimated optical depth ~4). Anti-Stokes channel transmission is 10%. Experimental repetition rate is 72 kHz. Statistical error bars represent averages of ~400,000 anti-Stokes detection events, corresponding to total averaging times of ~1 hour per point. Error bars, ±1 s.d.

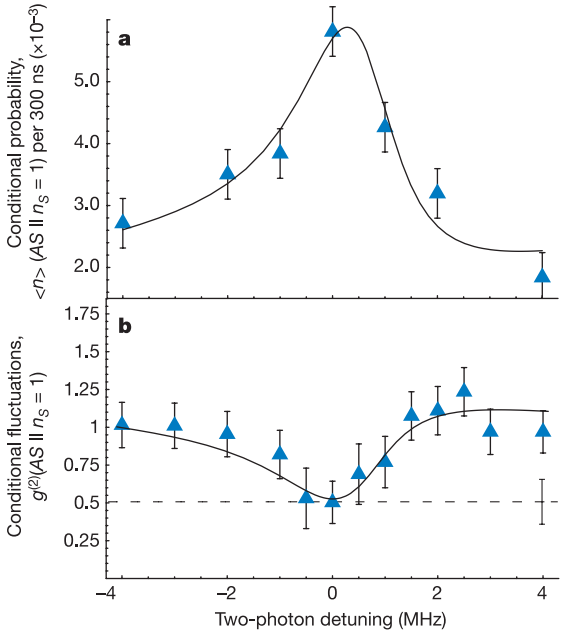


**Figure 3 | Observation of single-photon EIT. a**, Conditional probability (per 300 ns) of detecting an anti-Stokes photon transmitted through the target ensemble, $\langle n \rangle (AS||n_S = 1)$, versus the EIT two-photon detuning $\delta$. Background (detection probability with write laser off) has been subtracted for transmission data in Figs 3a and 4. For incident pulses, $\langle n \rangle (AS||n_S = 1) \approx 0.01$. **b**, Second-order correlation function of the anti-Stokes field conditioned on detecting one Stokes photon, $g^{(2)}(AS||n_S = 1)$, as a function of $\delta$. Dashed line and error bar represent measured value with no target ensemble present. For the data shown, $\delta$ is varied by varying the EIT control frequency. For these experiments, $p\eta_S \approx 0.06$, $\eta_S \approx 0.25$ and the (source, target) ensemble temperature ≈(26 °C, 30 °C). Overall probability per trial to detect anti-Stokes photons is $6 \times 10^{-3}$ for incident (target cell absent) photons and $3 \times 10^{-3}$ for transmitted (target cell present, $\delta = 0$) photons. Statistical error bars represent averages of ~1 million anti-Stokes detection events, corresponding to total averaging times of ~2 hours per point. The solid line results from the theoretical model described in the text; the parameter values used in the model (retrieve laser Rabi frequency = 35 MHz, retrieve laser detuning = 400 MHz, anti-Stokes background = 0.003 photons per pulse, optical depth = 2.5, single-photon bandwidth = 0.7 MHz, $|g\rangle$–$|s\rangle$ coherence decay = 0.02 MHz), are similar to experimental conditions. Error bars, ±1 s.d.

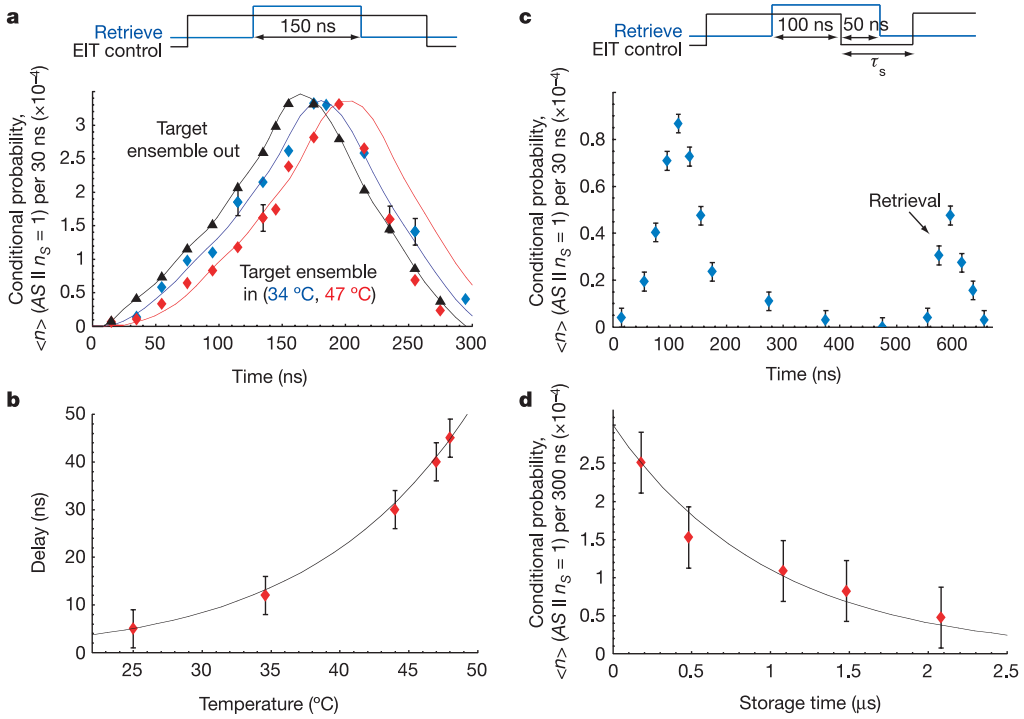


**Figure 4 | Time-resolved measurements of single-photon pulse delay and storage. a**, Conditional probability (per 30 ns) of detecting an anti-Stokes photon transmitted through the target ensemble. Target ensemble absent (black triangles); target ensemble present at 34.6 °C (blue diamonds) and 47 °C (red diamonds). Delayed pulse at (34.6 °C, 47 °C) is scaled by (1.34, 2.14). Solid lines represent theoretical calculations for EIT propagation in a Doppler-broadened medium. **b**, Delay, relative to free-space propagation, of single-photon anti-Stokes pulses, as a function of target-ensemble temperature. Solid line is a theoretical prediction for an EIT control field Rabi frequency of 35 MHz. **c**, Storage and retrieval of a single-photon anti-Stokes pulse. EIT control is turned off 100 ns after the retrieval from the source ensemble begins; after waiting for a storage time of $\tau_s = 460$ ns, the EIT control is turned back on, resulting in the retrieved pulse centred at 600 ns. Target ensemble temperature ~47 °C. **d**, Conditional probability (per 300 ns) of detecting an anti-Stokes photon retrieved from the target ensemble after storage interval $\tau_s$. $\langle n \rangle (AS \| n_S = 1) = 0.003$ for the incident pulse (measured with target ensemble absent). For short storage times, the overall probability per trial to detect (incident, retrieved) anti-Stokes photons is $\sim(1.5 \times 10^{-3}, 1.5 \times 10^{-4})$. Decay of probability is fitted by an exponential with a 1/e characteristic time of about 1 μs; this is consistent with diffusion of atoms from the detection volume. Error bars, ±1 s.d.

ensembles. Applications of quantum-optical processes involving simultaneous control over temporal, spectral, and quantum-statistical properties of single photons are possible[1,2,28,29]. For example, by storing polarization-encoded qubits either in a pair of atomic ensembles[20], or in a pair of different Zeeman sublevels[21], this technique can be used for exploring quantum-information concepts such as quantum networks[1] and repeaters[2]. At the same time, coherent nonlinear-optical interactions at the single-photon level have been proposed by combining these techniques with resonantly enhanced atomic nonlinearities[29].

**Received 2 September; accepted 13 October 2005.**


1. Briegel, H. J., Dur, W., van Enk, S. J., Cirac, J. I. & Zoller, P. in *The Physics of Quantum Information* (eds Bouwmeester, D., Ekert, A. & Zeilinger, A.) 281–293 (Springer, Berlin, 2000).
2. Duan, L. M., Lukin, M. D., Cirac, J. I. & Zoller, P. Long-distance quantum communication with atomic ensembles and linear optics. *Nature* **414,** 413–418 (2001).
3. Kuzmich, A. *et al.* Generation of nonclassical photon pairs for scalable quantum communication with atomic ensembles. *Nature* **423,** 731–734 (2003).
4. van der Wal, C. H. *et al.* Atomic memory for correlated photon states. *Science* **301,** 196–200 (2003).
5. McKeever, J. *et al.* Deterministic generation of single photons from one atom trapped in a cavity. *Science* **303,** 1992–1994 (2004).
6. Kuhn, A., Hennrich, M. & Rempe, G. Deterministic single-photon source for distributed quantum networking. *Phys. Rev. Lett.* **89,** 067901 (2002).
7. Julsgaard, B., Sherson, J., Cirac, J. I., Fiurasek, J. & Polzik, E. S. Experimental demonstration of quantum memory for light. *Nature* **432,** 482–486 (2004).
8. Harris, S. E. Electromagnetically induced transparency. *Phys. Today* **50,** 36–42 (1997).
9. Fleischhauer, M., Imamoglu, A. & Marangos, J. P. Electromagnetically induced transparency: Optics in coherent media. *Rev. Mod. Phys.* **77,** 633–673 (2005).
10. Hau, L. V., Harris, S. E., Dutton, Z. & Behroozi, C. H. Light speed reduction to 17 metres per second in an ultracold atomic gas. *Nature* **397,** 594–598 (1999).
11. Kash, M. M. *et al.* Ultraslow group velocity and enhanced nonlinear optical effects in a coherently driven hot atomic gas. *Phys. Rev. Lett.* **82,** 5229–5232 (1999).
12. Phillips, D. F., Fleischhauer, A., Mair, A., Walsworth, R. L. & Lukin, M. D. Storage of light in atomic vapor. *Phys. Rev. Lett.* **86,** 783–786 (2001).
13. Liu, C., Dutton, Z., Behroozi, C. H. & Hau, L. V. Observation of coherent optical information storage in an atomic medium using halted light pulses. *Nature* **409,** 490–493 (2001).
14. Longdell, J. J., Fraval, E., Sellars, M. J. & Manson, N. B. Stopped light with storage times greater than one second using electromagnetically induced transparency in a solid. *Phys. Rev. Lett.* **95,** 063601 (2005).
15. Braje, D. A., Balić, V., Yin, G. Y. & Harris, S. E. Low-light-level nonlinear optics with slow light. *Phys. Rev. A* **68,** 041801(R) (2003).
16. Chou, C. W., Polyakov, S. V., Kuzmich, A. & Kimble, H. J. Single-photon generation from stored excitation in an atomic ensemble. *Phys. Rev. Lett.* **92,** 213601 (2004).
17. Eisaman, M. D. *et al.* Shaping quantum pulses of light via coherent atomic memory. *Phys. Rev. Lett.* **93,** 233602 (2004).
18. Jiang, W., Han, C., Xue, P., Duan, L.-M. & Guo, G.-C. Nonclassical photon pairs generated from a room-temperature atomic ensemble. *Phys. Rev. A* **69,** 043819 (2004).
19. Balić, V., Braje, D. A., Kolchin, P., Yin, G. Y. & Harris, S. E. Generation of paired photons with controllable waveforms. *Phys. Rev. Lett.* **94,** 183601 (2005).
20. Matsukevich, D. N. & Kuzmich, A. Quantum state transfer between matter and light. *Science* **306,** 663–666 (2004).
21. Matsukevich, D. N. *et al.* Entanglement of a photon and a collective atomic excitation. *Phys. Rev. Lett.* **95,** 040405 (2005).
22. Mandel, L. & Wolf, E. *Optical Coherence and Quantum Optics* (Cambridge Univ. Press, Cambridge, 1995).
23. Michler, P. *et al.* A quantum dot single-photon turnstile device. *Science* **290,** 2282–2285 (2000).

24. Eisaman, M. D. *et al.* in *Fluctuations and Noise in Photonics and Quantum Optics III* Vol. 5,842 (eds Hemmer, P. R., Gea-Banacloche, J. R., Heszler, P. & Zubairy, M. S.) 105–113 (SPIE, Bellingham, Washington, 2005).
25. Fleischhauer, M. & Lukin, M. D. Dark-state polaritons in electromagnetically induced transparency. *Phys. Rev. Lett.* **84,** 5094–5097 (2000).
26. Akamatsu, D., Akiba, K. & Kozuma, M. Electromagnetically induced transparency with squeezed vacuum. *Phys. Rev. Lett.* **92,** 203602 (2004).
27. Black, A. T., Thompson, J. K. & Vuletić, V. On-demand superradiant conversion of atomic spin gratings into single photons with high efficiency. *Phys. Rev. Lett.* **95,** 133601 (2005).
28. Scully, M. O. & Ooi, C. H. R. Improving quantum microscopy and lithography via Raman photon pairs: II. *Analysis. J. Opt. B* **6,** S816–S820 (2004).
29. André, A., Bajcsy, M., Zibrov, A. S. & Lukin, M. D. Nonlinear optics with stationary pulses of light. *Phys. Rev. Lett.* **94,** 063902 (2005).
30. André, A. *Nonclassical States of Light and Atomic Ensembles: Generation and New Applications* PhD thesis, Harvard Univ. (2005).

**Acknowledgements** We acknowledge T. Zibrova, A. Gorshkov, P. Hemmer, J. MacArthur, D. Phillips and R. Walsworth for discussions and experimental help. This work was supported by DARPA, the Packard and Sloan Foundations, and the NSF through the CAREER programme and the Harvard-MIT Center for Ultracold Atoms.

**Author Information** Reprints and permissions information is available at npg.nature.com/reprintsandpermissions. The authors declare no competing financial interests. Correspondence and requests for materials should be addressed to M.D.E. (eisaman@fas.harvard.edu).